RJC

INHIBITION EFFECT OF ENVIRONMENTALLY BENIGN KUCHLA (*STRYCHNOS NUXVOMICA*) SEED EXTRACT ON CORROSION OF MILD STEEL IN HYDROCHLORIC ACID SOLUTION

Ambrish Singh[1], V. K. Singh[1], M. A. Quraishi [2],*

[1]Department of Chemistry, Udai Pratap Autonomous College, Varanasi 221002 (India)
[2]Department of Applied Chemistry, Institute of Technology
Banaras Hindu University, Varanasi 221005 (India)
*E-mail: maquraishi.apc@itbhu.ac.in

ABSTRACT

The inhibition of the corrosion of mild steel in hydrochloric acid solution by the seed extract of Kuchla (*Strychnos Nuxvomica*) has been studied using weight loss, electrochemical impedance spectroscopy, potentiodynamic polarization and linear polarization techniques. Inhibition was found to increase with increasing concentration of the extract. The effect of temperature, immersion time and acid concentration on the corrosion behavior of mild steel in 1 M HCl with addition of extract was also studied. The adsorption of the extract on the mild steel surface obeyed the Langmuir adsorption isotherm. Values of inhibition efficiency calculated from weight loss, potentiodynamic polarization, and electrochemical impedance spectroscopy (EIS) are in good agreement. Polarization curves showed that Kuchla (*Strychnos Nuxvomica*) seed extract behaves as a mixed-type inhibitor in hydrochloric acid. The activation energy as well as other thermodynamic parameters for the inhibition process was calculated. The adsorbed film on mild steel surface containing Kuchla (*Strychnos Nuxvomica*) seed extract inhibitor was also measured by Fourier transform infrared spectroscopy (FTIR). The results obtained showed that the seed extract of Kuchla (*Strychnos Nuxvomica*) could serve as an effective inhibitor of the corrosion of mild steel in hydrochloric acid media.

Keywords: Kuchla (*Strychnos Nuxvomica*); Corrosion inhibition; Mild steel; electrochemical measurement; FTIR

INTRODUCTION

Inhibitors are frequently used for controlling corrosion of metals and alloys in acidic media for removing scales and rusts in metal finishing industries, cleaning of boilers and heat exchangers. Use of inhibitors is one of the most practical methods for protection against corrosion especially in acid solutions to prevent unexpected metal dissolution and acid consumption[1, 2]. The known hazardous effect of most synthetic corrosion inhibitors have motivated scientists to use naturally occurring products as corrosion inhibitors as they are   inexpensive, readily available and renewable sources of materials, environmentally friendly and ecologically accepTable[3,4].

Up till now many plant leaves extracts such as *Murraya koenigii*, *Andrographis paniculata*, *Embilica officianilis*, *Terminalia chebula*, *Terminalia belivia, Sapindus trifolianus* , *Accacia conicianna* *,Swertia angustifolia. Eugenia jambolans*, *Pongamia glabra*, *Annona squamosa* *,Accacia Arabica* *,Occimum viridis, Telferia occidentalis, Carica papaya, Azadirachta indica* *Vernonia amydalina*, *Nypa fructicans* wurmb, *Ricimus communis* coriander*,* hibiscus, Eucalyptus, anis, black cumin and garden cress have been studied for the corrosion inhibition of mild steel in acid media[5-11]. Some of the seeds such as *Pongamia pinnata*, Tobacco, castor oil seeds, acacia gum and lignin along with *.Papaia*, *Poinciana pulcherrima*, *Cassia occidentalis* and *Datura stramonmium* have also been used as efficient corrosion inhibitor for steel[12-16].The anticorrosion activity of onion, garlic and bitter gourd for mild steel in acid media showed good results studied. Oil extracts of Ginger, jojoba, eugenol, acetyl-eugenol, *artemisia* oil and *Mentha pulegium* are used for corrosion inhibition of steel in acid media[17,18].Saps of certain plants is very useful

corrosion inhibitors. *Calotropis procera, Azydracta indica* and *Auforpio turkiale* sap are useful as acid corrosion inhibitors. Quinine has been studied for its anticorrosive effect of carbon steel in 1 M HCl. The inhibition effect of *Zenthoxylum alatum* extract on the corrosion of mild steel in aqueous Orthophosphonic acid was investigated[19].

In continuation of our work on development of green corrosion inhibitors[20-23], the present study investigates the inhibiting effect of seed extract of *Strychnos Nuxvomica*, which is commonly known as Kuchla in India. Inhibition effect of Kuchla (*Strychnos Nuxvomica*) on the corrosion of mild steel in 1 M HCl solution by weight loss, potentiodynamic polarization and electrochemical impedance spectroscopy (EIS) methods. Meanwhile, the steel surface was examined by Fourier transform infrared (FTIR) spectroscopy.

EXPERIMENTAL

Preparation of Kuchla (Strychnos Nuxvomica) seed extract

Kuchla (*Strychnos Nuxvomica*) seed was dried and ground to powder form. Dried (10g) powder was soaked in double distilled water (500 mL) and refluxed for 5 h. The aqueous solution was filtered and concentrated to 100 mL .This extract was used to study the corrosion inhibition properties. Corrosion tests were performed on a mild steel of the following percentage composition (wt.%): Fe 99.30%, C 0.076%, Si 0.026%, Mn 0.192%, P 0.012%, Cr 0.050%, Ni 0.050%, Al 0.023%, and Cu 0.135% , which were abraded successively with fine grade emery papers from 600 to 1200 grade. The specimens were washed thoroughly with double distilled water and finally degreased with acetone and dried at room temperature. The aggressive solution 1 M HCl was prepared by dilution of analytical grade HCl (37%) with double distilled water and all experiments were carried out in unstirred solutions.

Weight loss method

Weight loss measurements were performed on the mild steel samples with a rectangular form of size 2.5 cm × 2.0 cm × 0.025 cm in one molar HCl solution with and without addition of different concentrations of seed's extract. Every sample was weighed by an electronic balance, and then placed in the acid solution (100 mL). The duration of the immersion was 3 h at the temperature range from 308 to 338 K. After immersion, the surface of the specimen was cleaned by double distilled water followed rinsing with acetone and the sample was weighed again in order to calculate inhibition efficiency (η %) the corrosion rate (C_R). The experiments were done in triplicate and the average value of the weight loss was noted. For each experiment, a freshly prepared solution was used and the solution temperature was thermostatically controlled at a desired value.

The aggressive solutions (1 M HCl) were prepared by dilution of an analytical grade HCl with double distilled water. The surface coverage (θ) and inhibition efficiency ((η %) was determined by using following equation:

$$\theta = \frac{w_0 - w_i}{w_0} \tag{1}$$

$$\eta\% = \frac{w_0 - w_i}{w_0} \times 100 \tag{2}$$

Where, w_i and w_0 are the weight loss values in presence and absence of inhibitor, respectively.
The corrosion rate (C_R) of mild steel was calculated using the relation:

$$C_R \, (mm / y) = \frac{87.6 \times w}{atD} \tag{3}$$

Where, w is corrosion weight loss of mild steel (mg), a the area of the coupon (cm^2), t is the exposure time (h) and D the density of mild steel (g cm^{-3}).

Electrochemical measurements

The electrochemical studies were made using a Gamry three electrode cell assembly at room temperature. The mild steel of 1 cm^2 was the working electrode, platinum electrode was used as an auxiliary electrode, and standard calomel electrode (SCE) was used as reference electrode. The working electrode was abraded with different grades of emery papers, washed with water and degreased with acetone. All

electrochemical measurements were carried out using Gamry Potentiostat/Galvanostat (Model G-300) with EIS software Gamry Instruments Inc., USA. Gamry applications include software DC 105 for corrosion and EIS 300 for EIS measurements and Echem Analyst version 5.50 software packages for data fitting. Prior to the electrochemical measurement, a stabilization period of 30 minute was allowed, which was proved to be sufficient to attain a sTable value of $E_{corr.}$

The linear polarization study was carried out from cathodic potential of – 20 mV versus OCP to an anodic potential of + 20 mV versus OCP with a sweep rate 0.125 mV s^{-1} to determine the polarization resistance (R_p).From the measured polarization resistance value, the inhibition efficiency has been calculated using the relationship:

$$\eta\% = \frac{R_p^{'} - R_p^{0}}{R_p^{'}} \times 100 \tag{4}$$

Where, R_p^{0} and $R_p^{'}$ are the polarization resistance in absence and in presence of inhibitor, respectively.

Tafel curves were obtained by changing the electrode potential automatically from −250 to +250 mV versus corrosion potential (E_{corr}) at a sweep rate of 1 mV s^{-1}. EIS measurements were carried out in a frequency range from 100 kHz to 10 mHz under potentiodynamic conditions, with amplitude of 10 mV peak-to-peak, using AC signal at E_{corr}. The linear Tafel segments of anodic and cathodic curves were extrapolated to corrosion potential to obtain corrosion current densities (I_{corr}). The inhibition efficiency was evaluated from the measured I_{corr} values using the relationship:

$$\eta\% = \frac{I_{corr}^{0} - I_{corr}^{'}}{I_{corr}^{0}} \times 100 \tag{5}$$

Where, I_{corr}^{0} and I_{corr}^{i} are the corrosion current in absence and in presence of inhibitor, respectively. The charge transfer resistance values were obtained from the diameter of the semi circles of the Nyquist plots. The inhibition efficiency of the inhibitor has been found out from the charge transfer resistance values using the following equation:

$$\eta\% = \frac{R_{ct}^{'} - R_{ct}^{0}}{R_{ct}^{'}} \times 100 \tag{6}$$

Where, R_{ct}^{0} and $R_{ct}^{'}$ are the charge transfer resistance in absence and in presence of inhibitor, respectively. All electrochemical measurements were done in unstirred and non de-aerated solutions.

Fourier transform infrared spectroscopy (FTIR)
FTIR spectra were recorded in a Thermo Nicolet-5700 FTIR spectrophotometer (USA). The mild steel specimens of size 2.5 cm × 2.0 cm × 0.025 cm were prepared as described above. These specimens were immersed for 3 h in 100 mL of 1 M HCl solution containing 350 ppm of inhibitor and were then dried. In order to prevent damage of the protective film or layer of the mild steel surfaces, the FTIR reflectance accessory was applied to study the mild steel surfaces.

RESULTS AND DISCUSSION

Weight loss Studies

Effect of Inhibitor concentration
Figure 1a represents the effect of inhibitor concentration on inhibition efficiency in HCl. The extract showed maximum inhibition efficiency of 98% in HCl and at a optimum concentration of 350 ppm .Further increase in extract concentration did not cause any significant change in the performance of the extract. The values of percentage inhibition efficiency ((η %) and corrosion rate (C_R) obtained from weight loss method at different concentrations of Kuchla (*Strychnos Nuxvomica*) seed extract at 308 K are summarized in Table 1.

Effect of immersion time

In order to assess the stability of inhibitive behaviour of seed extract on a time scale, weight loss measurements were performed in 1 M HCl in absence and presence of seed extract at 350 ppm concentration for 2 to 8 h immersion time at temperature 308 K. Inhibition efficiencies were plotted against immersion time as seen from Figure 1b. This figure shows that inhibition efficiency of the extract was increased with increasing immersion time from 2 to 8 h (give values). The increase in inhibition efficiency upto 8 h reflects the strong adsorption of constituents present in the extract on the mild steel surface, resulting in a more protective layer formed at mild steel/hydrochloric acid solution interface. Thus Kuchla (*Strychnos Nuxvomica*) seed extract effectively inhibit the mild steel corrosion in one molar hydrochloric acid solutions.

Effect of acid concentration

The variation of inhibition efficiency with increase in acid concentration from 0.5 M to 2 M is shown in Figure 1c. From this figure it can be seen that inhibition efficiency decreases from 98% to 82% with increase in HCl concentration from 0.5 M to 2 M. This decrease in efficiency ((η %) can be attributed to increased aggressiveness of solutions with increase in acid concentration.

Effect of temperature

To evaluate the stability of adsorbed layer/film of inhibitor on mild steel surface as well as activation parameters of the corrosion process of steel in acidic medium, weight loss measurements were carried out in the range of temperature 308-338 K in the absence and presence of extract at optimum concentration during 3 h immersion time. Results thus obtained are shown in Figure1d. It is evident from this Figure 1d that inhibition efficiency decreases with increasing temperature. This is due to increased rate of dissolution process of mild steel and partial desorption of the inhibitor from the metal surface with temperature[24].

The log of corrosion rate is a linear function of temperature (Arrhenius equation)[25-27]:

$$\log(C_R) = \frac{-E_a}{2.303RT} + A \tag{7}$$

where, E_a is the apparent effective activation energy, R is the general gas constant and A is Arrhenius pre exponential factor. A plot of log of corrosion rate obtained by weight loss measurement versus $1/T$ gave a straight line as shown in Figure 2a with a slope of $-E_a / 2.303\,R$. The values of activation energy are listed in Table 2. The data shows that the activation energy (E_a) of the corrosion in mild steel in 1 M HCl solution in the presence of extract is higher than that in the free acid solution. The increase in the apparent activation energy for mild steel dissolution in inhibited solution may be interpreted as physical adsorption that occurs in the first stage[28]. Szauer and Brand explained[29] that the increase in activation energy can be attributed to an appreciable decrease in the adsorption of the inhibitor on the mild steel surface with increase in temperature. An alternative formulation of Arrhenius equation is[30]:

$$C_R = \frac{RT}{Nh} \exp\left(\frac{\Delta S^*}{R}\right) \exp\left(\frac{-\Delta H^*}{RT}\right) \tag{8}$$

where, h is plank's constant, N is Avogadro's number, ΔS^* the entropy of activation, and ΔH^* the enthalpy of activation. A plot of log C_R/T versus $1/T$ gave a straight line (Figure 2b) with a slope equal to $-\Delta H^*/2.303\,R$ and an intercept of log $R/N\,h + \Delta S^*/2.303\,R$, from which the values of ΔS^* and ΔH^* were calculated and listed in Table 2. The positive signs of enthalpies (ΔH^*) reflect the endothermic nature of dissolution process. This suggests that mild steel dissolution requires more energy in 1 M HCl in the presence of seed extract. The shift towards positive value of entropies(ΔS^*) imply that the activated complex in the rate determining step represents dissociation rather than association, meaning that disordering increases on going from reactants to the activated complex[31].

EIS Measurement

Impedance spectra for mild steel in 1 M HCl in absence and presence of different concentrations of Kuchla (*Strychnos Nuxvomica*) seed extract are shown in the form of Nyquist plots (Figure 3a), Bode-

modulus plots (Figure 3b) and Bode plots in the Theta-frequency format (Figure 3c). It can be seen from Figs. 3 that diameter of the semicircular capacitive loop (Figure 3a), and phase angle (Figure 3c) increased with increasing concentration of seed extract, and impedance of the double layer (Figure 3b) decreased with extract concentration. Nyquist plots consist of a "depressed" semicircle with one capacitive loop and depressed semicircle has a centre under the real axis. Such behaviour is characteristic for solid electrodes and often referred to as frequency dispersion and has been attributed to roughness and other inhomogeneities of solid surface[32, 33]. The Nyquist plots show a depressed capacitive loop in the high frequency (HF) range and an inductive loop in the lower frequency (LF) range. The HF capacitive loop can be attributed to the charge transfer reaction and time constant of the electric double layer and to the surface inhomogeneity of structural or interfacial origin, such as those found in adsorption processes[34]. The LF inductive loop may be attributed to the relaxation process obtained by adsorption species like Cl^-_{ads} and H^+_{ads} on the electrode surface and might also be attributed to the re-dissolution of the passivates surface at low frequencies. The fact that this semicircle cannot be observed after the addition of higher concentration supports our view[35, 36].

The impedance spectra for Nyquist plots were analyzed by fitting to the equivalent circuit model (Figure 4) which was used elsewhere to describe iron / acid interface[37]. In this equivalent circuit, R_s is the solution resistance, R_{ct} is the charge transfer resistance and CPE is a constant phase element. The capacitance values were calculated using the equation[38]:

$$Z_{CPE} = Q^{-1}(j\omega)^{-n}$$
(9)

where Q is the *CPE* constant, j is the imaginary unit, ω is the angular frequency ($\omega = 2\pi f$, the frequency in Hz), and n is the *CPE* exponent which can be used as a gauge of the heterogeneity and gives details about the degree of surface inhomogeneity (roughness). Depending on the value of n, CPE can represent resistance ($n = 0$, $Q = 1/R$), capacitance ($n = 1$, $Q = C$), inductance ($n = -1$, $Q = 1/L$) or Warburg element ($n = 0.5$).

When $n = 1$, this is the same equation as that for the impedance of a capacitor, where $Q = C_{dl}$. In fact, when n is close to 1, the *CPE* resembles a capacitor, but the phase angle is not 90°. It is constant and somewhat less than 90° at all frequencies.

In spite of the mentioned fact, the term, double layer capacitance, is still often used in the evaluation of AC impedance results to characterize the double layer believed to be formed at the metal/solution interface of systems displaying non-ideal capacitive behavior. For providing simple comparison between the capacitive behaviors of different corrosion systems, the values of Q were converted to C_{dl}.

$$C_{dl} = Q(\omega_{max})^{n-1}$$
(10)

here, ω_{max} represents the frequency at which the imaginary component reaches a maximum. It is the frequency at the top of the depressed semicircle, and it is also the frequency at which the real part (Z_r) is midway between the low and high frequency x-axis intercepts.

The impedance parameters such as solution resistance (R_s), charge transfer resistance (R_{ct}), Q, n, derived double layer capacitance (C_{dl}) and inhibition efficiency ((η %) are listed in Table 3. The values of η % are calculated using the following equation:

$$\eta(\%) = \frac{R_{ct,i} - R_{ct,0}}{R_{ct,i}} \times 100$$
(11)

where, $R_{ct,i}$ and $R_{ct,0}$ are charge transfer resistances in presence and absence of inhibitor, respectively. It is clear from Table 3 that by increasing the inhibitor concentration, the C_{dl} values tend to decrease and the inhibition efficiency increases. The decrease in C_{dl} values can be attributed to a decrease in local dielectric constant and / or an increase in the thickness of the electrical double layer, suggesting that Kuchla (*Strychnos Nuxvomica*) seed extract act by adsorption at the mild steel / solution interface[39]. On the other hand, the values of C_{dl} decreased with an increase in the extract concentration. This situation was the result of an increase in the surface coverage by the inhibitor, which led to an increase in the inhibition efficiency. The values of the phase shift indicate that the C_{dl} values are in reasonable

confidence limit. Also any significant change in the values of the phase shift, *n*, was not observed in the absence and in the presence of Kuchla (*Strychnos Nuxvomica*). To predict the dissolution mechanism, the value of *n* can be used as an indicator[40]. The values of *n*, ranging between 0.827 and 0.855, indicate that the charge transfer process controls the dissolution mechanism of mild steel in one molar HCl solution in the absence and in the presence of seed extract. The thickness of the protective layer, δ_{org}, was related to C_{dl} by the following equation[41].

$$\delta_{org} = \frac{\varepsilon_0 \varepsilon_r}{C_{dl}} \qquad (12)$$

where, ε_0 is the dielectric constant and ε_r is the relative dielectric constant. This decrease in the C_{dl}, which can result from a decrease in local dielectric constant and/or an increase in the thickness of the electrical double layer, suggested that Kuchla (*Strychnos Nuxvomica*) seed extract function by adsorption at the metal/solution interface. Thus, the change in C_{dl} values was caused by the gradual replacement of water molecules by the adsorption of the organic molecules on the metal surface, decreasing the extent of metal dissolution [42].
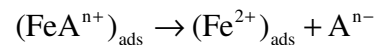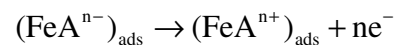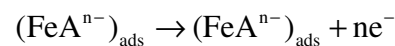
It is apparent from Nyquist plots that the impedance response of mild steel in inhibited HCl solution has significantly changed after the addition of Kuchla (*Strychnos Nuxvomica*) seed extract in acid solution and that the impedance of inhibited substrate increases with increasing conc. of inhibitor. The Nyquist plots showed that on increasing Kuchla (*Strychnos Nuxvomica*) concentration, increases charge transfer resistance and decreases double layer capacitance. From the Table 3, it is clear that the greatest effect was observed at 350 ppm of Kuchla (*Strychnos Nuxvomica*) extract which gives R_{ct} value of 264 Ωcm^2 in 1 M HCl respectively. Inhibition efficiency is found to increase with inhibitor concentration in the acid .The data obtained from EIS are in good agreement with those obtained from weight loss method.
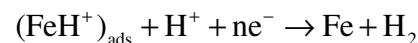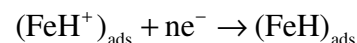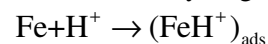
Polarization Measurements

Polarization curves for mild steel at various concentration of Kuchla (*Strychnos Nuxvomica*) seed extract in aerated solutions are shown in Figure 5. The extrapolation of Tafel straight line allows the calculation of the corrosion current density (I_{corr}). The values of I_{corr}, the corrosion potential (E_{corr}), cathodic and anodic Tafel slopes (b_c, b_a) and inhibition efficiency *(η %)* are given in Table 4.The *(η %)* is calculated using the following equation:

$$\eta\% = \left(\frac{I_{corr}^0 - I_{corr}^i}{I_{corr}^0} \right) \times 100 \qquad (13)$$

Where, I_{corr}^0 and I_{corr}^i are the corrosion current density values without and with inhibitor, respectively. Some of the authors proposed the following mechanism for the corrosion of iron and steel in acid solution[43-45]:

$$Fe + A^{n-} \rightarrow (FeA^{n-})_{ads}$$

$$(FeA^{n-})_{ads} \rightarrow (FeA^{n-})_{ads} + ne^-$$

$$(FeA^{n-})_{ads} \rightarrow (FeA^{n+})_{ads} + ne^-$$

$$(FeA^{n+})_{ads} \rightarrow (Fe^{2+})_{ads} + A^{n-}$$

The cathodic hydrogen evolution

$$Fe + H^+ \rightarrow (FeH^+)_{ads}$$

$$(FeH^+)_{ads} + ne^- \rightarrow (FeH)_{ads}$$

$$(FeH^+)_{ads} + H^+ + ne^- \rightarrow Fe + H_2$$

The change in b_a and b_c values as shown in Table 4 indicates that adsorption of Kuchla (*Strychnos Nuxvomica*) seed extract modify the mechanism of anodic dissolution as well as cathodic hydrogen evolution. From the Figure 5, it is clear that both the cathodic and anodic reactions are inhibited and the inhibition increases as the inhibitor conc. increases in acid media, but the cathode is more polarized. From

the Table 4, it is clear that there was no definite trend in the shift of E_{corr} values, in the presence of various conc. of Kuchla (*Strychnos Nuxvomica*) seed extract in 1 M HCl solution. This result indicated that Kuchla (*Strychnos Nuxvomica*) seed extract can be classified as mixed type of inhibitor in 1 M HCl solution.

Adsorption Isotherm and free energy of adsorption

The adsorption of an organic adsorbate on to metal-solution interface can be represented by a substitutional adsorption process between the organic molecules in the aqueous solution phase ($Org_{(sol)}$) and the water molecules on the metallic surface ($H_2O_{(ads)}$)[46].

$$Org_{(sol)} + xH_2O \rightarrow Org_{(ads)} + xH_2O_{(sol)} \qquad (14)$$

where, x is the size ratio representing the number of water molecules replaced by one molecule of organic adsorbate. Basic information on the interaction between the inhibitor and the mild steel surface can be provided by the adsorption isotherm. For this purpose, the values of surface coverage (θ) at different concentrations (C_{inh}) of Kuchla (*Strychnos Nuxvomica*) seed extract in acid media in the temperature range (308-338 K) have been used to explain the best isotherm to determine the adsorption process. The values of θ can be easily determined from the ratio *((η %) /100)*, where *(η %)* was obtained from weight loss measurements. Attempts were made to fit these θ values to various isotherm including Frumkin, Langmuir, Temkin. According to these isotherms, θ is related to the inhibitor concentration, C_{inh}:

$$\theta = \frac{bC_{inh}}{1+bC_{inh}} \qquad \text{(Langmuir isotherm)} \qquad (15)$$

$$\exp(-2a\theta) = K_{ads}C_{inh} \qquad \text{(Temkin isotherm)} \qquad (16)$$

where, b designates the adsorption coefficient in equation (15), a the molecular interaction parameter, K_{ads} is the equilibrium constant of the adsorption process in equation (16). The best fit was obtained with Langmuir isotherm as shown in Figure 6. The value of regression coefficients ($R^2 = 0.999$) confirms the validity of this approach.

Fourier transform infrared spectroscopy (FTIR) analysis

It has been established that FTIR spectrophotometer is a powerful instrument that can be used to determine the type of bonding for organic inhibitors absorbed on the metal surface. In present study, reflectance FTIR spectra were used to support the fact that corrosion inhibition of mild steel in acid media is due to the adsorption of inhibitor molecules on the mild steel surface. The prominent peaks are given in Table 5. From data in Table 5, it can be established that inhibition of corrosion of mild steel in one molar HCl solution by Kuchla (*Strychnos Nuxvomica*) seed extract was due to the adsorption of extract's constituent on the mild steel surface.

Mechanism of inhibition

The transition of metal/solution interface from a state of active dissolution to the passive state is attributed to the adsorption of the inhibitor molecules at the metal/solution interface, forming a protective film. The rate of adsorption is usually rapid and hence, the reactive metal surface is shielded from the aggressive environment[47].

Adsorption process can occur through the replacement of solvent molecules from metal surface by ions and molecules accumulated in the vicinity of metal/solution interface. Ions can accumulate at the metal/solution interface in excess of those required to balance the charge on the metal at the operating potential. These ions replace solvent molecules from the metal surface and their centers reside at the inner Helmholtz plane. This phenomenon is termed specific adsorption, contact adsorption. The anions are adsorbed when the metal surface has an excess positive charge in an amount greater than that required to balance the charge corresponding to the applied potential. Aromatic compounds (which contain the benzene ring) undergo particularly strong adsorption on many electrode surfaces. The bonding can occur between metal surface atoms and the aromatic ring of the adsorbate molecules or ligands substituent groups. The exact nature of the interactions between a metal surface and an aromatic molecule depends on the relative coordinating strength towards the given metal of the particular groups present[48].

The main constituent of extract of Kuchla (*Strychnos Nuxvomica*) seed is Brucine whose structure is given in Figure 7. *Strychnos nuxvomica* showed good performance owing to the presence of three methoxy group directly attached to the benzene nucleus in its structure. The presence of methoxy group greatly enhanced the electron density of benzene ring which favors its greater adsorption on the mild steel surface, thereby giving rise in very high inhibiting performance (98%) at a concentration as 350 ppm.

It is not possible to consider a single adsorption mode between inhibitor and metal surface because of the complex nature of adsorption and inhibition of a given inhibitor. The adsorption of main constituents of seed extract can be attributed to the presence of O-atoms, π- electrons and aromatic/heterocyclic rings. Presence of methoxy group also enhances the inhibition efficiency.Therefore, the possible reaction centres are unshared electron pair of hetero-atoms and π- electrons of aromatic/heterocyclic ring. In aqueous acidic solutions, main constituents exist either as neutral molecules or as protonated molecules (cations). The inhibitors may adsorb on the metal/acid solution interface by one and/or more of the following ways: (i) electrostatic interaction of protonated molecules with already adsorbed chloride ions, (ii) donor-acceptor interactions between the π-electrons of aromatic ring and vacant d orbital of surface iron atoms, (iii) interaction between unshared electron pairs of hetero atoms and vacant d-orbital of iron surface atoms.

Generally two modes of adsorption are considered on the metal surface in acid media. In one mode, the neutral molecules may be adsorbed on the surface of mild steel through the chemisorption mechanism, involving the displacement of water molecules from the mild steel surface and the sharing electrons between the hetero atoms and iron. The inhibitor molecules can also adsorb on the mild steel surface on the basis of donor–acceptor interactions between π-electrons of the aromatic/heterocyclic ring and vacant d-orbitals of surface iron atoms. In second mode, since it is well known that the steel surface bears positive charge in acid solution[49], so it is difficult for the protonated molecules to approach the positively charged mild steel surface (H_3O^+/metal interface) due to the electrostatic repulsion. Since chloride ions have a smaller degree of hydration, thus they could bring excess negative charges in the vicinity of the interface and favour more adsorption of the positively charged inhibitor molecules, the protonated inhibitors adsorb through electrostatic interactions between the positively charged molecules and the negatively charged metal surface. Thus there is a synergism between adsorbed Cl^- ions and protonated inhibitors. Thus inhibition of mild steel corrosion in one molar HCl is due to the adsorption of extract constituents on the mild steel surface. This assumption could be further confirmed by the reflectance FTIR analysis of mild steel surface.

CONCLUSIONS

1. Kuchla (*Strychnos Nuxvomica*) seed extract is a good inhibitor for mild steel corrosion in one molar HCl solution. Inhibition efficiency increases with increasing seed extract concentration and *η* % values obtained from different methods employed are in reasonable agreement.
2. The adsorption of Kuchla (*Strychnos Nuxvomica*) seed extract on mild steel surface obeyed Langmuir adsorption isotherm.
3. Polarization curves measurements indicate that Kuchla (*Strychnos Nuxvomica*) seed extract acted as mixed type inhibitor.
4. The increasing value of CPE exponent i.e. the phase shift (*n*) with increasing inhibitor concentration indicated that surface roughness decreased with increasing inhibitor concentration.
5. The reflectance FTIR analysis showed that the inhibition of mild steel corrosion occurred due to the formation of a protective film on the metal surface through adsorption of constituents of Kuchla (*Strychnos Nuxvomica*) seed extract.

REFERENCES

1. H. Ashassi-Sorkhabi, D. Seifzadeh and M.G. Hosseini, *Corros. Sci*., **50,** 3363 (2008)
2. A.K. Satapathy, G. Gunasekaran, S.C. Sahoo, A. Kumar and P.V. Rodrigues, *Corros. Sci*., **51**, 2848 (2009).
3. A.M. Abdel-Gaber, B.A. Abd-El-Nabey and M. Saadawy, *Corros. Sci*., **51**, 1038 (2009)
4. P.B. Raja and M.G. Sethuraman, *Mater. Lett.*, **62**, 113 (2008).

5. E.A. Noor, *J. Engg. Appl. Sci*., **3,** 23(2008)
6. J. Buchweishaija and G.S. Mhinzi, *Port. Electrochim. Acta*., **26,** 257 (2008).
7. A.K. Satapathy, G. Gunasekaran, S.C. Sahoo, Kumar Amit and P.V. Rodrigues, *Corros. Sci.*, **51**, 2848 (2009).
8. Gregory O. Avwiri and F.O. Igho, *Mater. Lett.,* **57**, 3705 (2003).
9. L. Valek and S. Martinez, *Mater. Lett.,* **61**, 148 (2007).
10. E.E. Oguzie, *Corros. Sci.,* **50,** 2993 (2008).
11. P.C. Okafor, M.E. Ikpi, I.E. Uwah, E.E. Ebenso, U.J. Ekpe and S.A. Umoren *Corros. Sci.,* **50**, 2310 (2008).
12. E.A. Noor, *J.Appl. Electrochem.,* **39**, 1465 (2009).
13. F.S. De Souza and A. Spinelli, *Corros. Sci.,* **51**, 642 (2009).
14. P.B. Raja and M.G. Sethuraman, *Mater. Lett*., **62**, 1602 (2008).
15. A.Y. El-Etre, *Corros. Sci.,* **45**, 2485(2003).
16. A.M. Badiea and K.N. Mohana, *J. Mater. Eng. Perform.,* **18**, 1264 (2009).
17. L.R. Chauhan and G. Gunasekaran, *Corros. Sci.,* **49**, 1143 (2007).
18. A.Y. El-Etre, M. Abdallah and Z.E. El-Tantawy, *Corros. Sci.,* **47**, 385 (2005).
19. Ambrish Singh, V.K. Singh and M.A. Quraishi, *J. Mater. Environ. Sci,.* **1** , 162 (2010)
20. Ambrish Singh, I. Ahamad, V. K. Singh and M.A. Quraishi, *J. Solid. State. Electr.,* DOI: 10.1007/s10008-010-1172-z, (2010).
21. M.A. Quraishi, Dileep Kumar Yadav and Ishtiaque Ahamad, *The Open Corrosion Journal.,* **2,** 56 (2009).
22. M.A. Quraishi, Ambrish Singh, Vinod Kumar Singh, Dileep Kumar Yadav and Ashish Kumar Singh, *Mater. Chem. Phy.,* **122**, 114 (2010).
23. Ambrish Singh, V.K. Singh and M.A. Quraishi, *International. J. of Corrosion.,* doi:10.1155/2010/275983, (2010).
24. M. Schorr and J. Yahalom, *Corros. Sci.,* **12,** 867 (1972).
25. M.A. Quraishi, S. Khan, *Ind. J. Chem. Technol.,* **12**, 576 (2005).
26. C.B. Breslin and W.M. Carrol, *Corros. Sci.,* **34**, 327 (1993).
27. M.G.A. Khedr and M.S. Lashien, *Corros. Sci.,* **33**, 137 (1992).
28. L. Larabi, O. Benali and Y. Harek, *Mater. Lett.,* **61**, 3287 (2007).
29. T. Szauer and A. Brandt, *Electrochim. Acta.,* **26**, 1253 (1981).
30. J.O.M. Bockris and A.K.N. Reddy, *Modern Electrochemistry*, Plenum Press, New York, (1977).
31. R.A. Prabhu, A.V. Shanbhag and T.V. Venkatesha, *J. Appl. Electrochem.,* **37**, 491 (2007).
32. M. Elayyachy, A. Idrissi and B. Hammouti, *Corros. Sci.,* **48**, 2470 (2006).
33. S. Martinez and M. Metikos-Hukovic, *J. Appl. Electrochem.,* **33**, 1137 (2003).
34. R.S. Goncalves, D.S. Azambuja and A.M. Serpa Lucho, *Corros. Sci.,* **44**, 467(2002).
35. M.A. Amin, S.S. Abd El-Rehim, E.E.F. El-Sherbini and R.S. Bayyomi, *Electrochim. Acta.,* **52**, 3588 (2007).
36. M. Kedam, O.R. Mattos and H. Takenouti, *J. Electrochem. Soc.,* **128**, 257 (1981).
37. F. Mansfeld, *Corrosion.,* **36,** 301 (1981).
38. J. Shukla and K.S. Pitre, *Corros. Rev.,* **20,** 217 (2002).
39. A. Yurt, G. Bereket, A. Kivrak, A. Balaban and B. Erk, *J. Appl. Electrochem.,* **35**, 1025 (2005).
40. A.A. Hermas, M.S. Morad and M.H. Wahdan, *J. Appl. Electrochem.,* **34**, 95 (2004).
41. F. Bentiss, B. Mehdi, B. Mernari, M. Traisnel and H. Vezin, *Corrosion.,* **58,** 399 (2002).
42. R.R. Anand, R.M. Hurd and N. Hackerman, *J. Electrochem. Soc.,* **112**, 138 (1965).
43. M.S. Morad and A.M.K. El-Dean, *Corros. Sci*., **48**, 3398 (2006).
44. K. Tebbji, B. Hammouti, H. Oudda, A. Ramdani and M. Benkadour, *Appl. Surf. Sci.,* **252**, 1378 (2005).
45. A. Yurt, A Balaban, S. Ustun Kandemir, G. Bereket and B. Erk, *Mater. Chem.Phy.,* **85**, 420 (2004).

46. G.K. Gomma and M.H. Wahdan, *Mater. Chem. Phy.*, **39**, 142 (1994).
47. C.Y. Chao, L.F. Lin and D.D. Macdonald *J. Electrochem. Soc.*, **128**, 1187 (1981).
48. I.M. Ritchie, S. Bailey and R. Woods, *Adv. Colloid Interface Sci.,* **80**, 183 (1999).
49. G. Trabenelli and F. Mansfeld, *Corrosion Mechanisms*., Marcel Dekker, New York,109, (1987).

[RJC-684/2010]

Table-1: Corrosion parameters for mild steel in aqueous solution of 1 M HCl in presence and absence of different concentrations of Kuchla (*Strychnos Nuxvomica*) seed extract from weight loss measurements at 308 K for 3 h

Inhibitor concentration (ppm)	Weight loss (mg cm^{-2})	η (%)	C_R (mm y^{-1})
1 M HCl	20.9	-	77.9
100	5.6	73	20.7
150	4.7	78	17.4
200	2.3	89	8.5
250	1.1	94	4.0
300	0.9	96	3.3
350	0.4	98	1.4

Table -2: The values of activation parameters E_a, ΔH^*_a, ΔS^*_a for mild steel in 1 M HCl in the absence and presence of optimum concentrations of Kuchla (*Strychnos Nuxvomica*) seed extract

Inhibitor conc. (ppm)	E_a (kJ mol^{-1})	ΔH^*_a (kJ mol^{-1})	ΔS^*_a (J K^{-1}mol^{-1})	ΔQ (kJ mol^{-1})
1 M HCl	28	22	-136	-
350 ppm	93	90	60	75

Table-3: Electrochemical impedance parameters for mild steel in 1 M HCl in absence and presence of different concentrations of Kuchla (*Strychnos Nuxvomica*) seed extract:

Acid Solution	Inhibitor (ppm)	R_s (Ω cm^2)	R_{ct} (Ω cm^2)	Q (Ω^{-1} s^n cm^{-2})	n (μF cm^{-2})	C_{dl}	η (%)
1 M HCl	0	1.2	9	250	0.827	67	-
	250	1.3	130	111	0.845	52	94
	300	1.4	160	97	0.835	47	95
	350	1.2	264	82	0.855	43	97

Table-4: Potentiodynamic polarization parameters for mild steel without and with different concentrations of Kuchla (*Strychnos Nuxvomica*) seed extract in 1 M HCl

Conc. of inhibitor (ppm)	Tafel data					Linear polarization data	
	E_{corr} (mV vs SCE)	I_{corr} (μA cm^{-2})	β_a (mV dec^{-1})	β_c (mV dec^{-1})	η (%)	R_p (Ω cm^2)	η (%)
1 M HCl	-446	1540	90	121	-	10	-
250	-461	132	62	125	91	121	92
300	-463	97	64	122	94	140	93
350	-494	28	55	106	98	308	97

Table-5: Prominent peaks obtained from reflectance FTIR spectroscopy

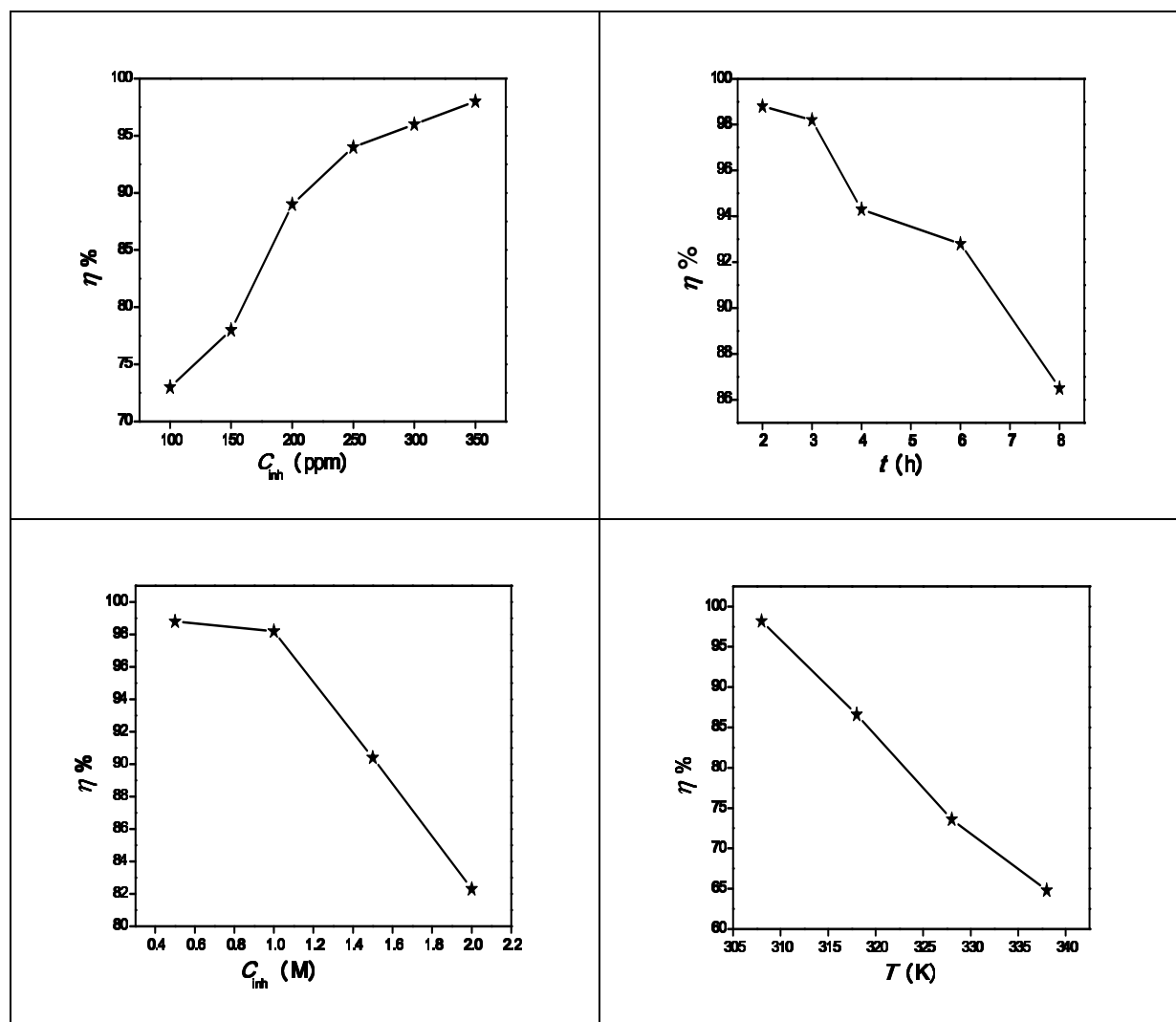| Frequency (cm^{-1})	Band assignment
1002	C–O stretching
1223	C–O stretching
1529, 1371	C=C (aromatic)
1650	C=O stretching
3159, 3054	Ar–H stretching
3973, 3880	Fe–O bending

Fig.-1: Variation of inhibition efficiency of Kuchla (*Strychnos Nuxvomica*) extracts in one molar HCl with (a) extract concentration, (b) immersion time, (c) acid concentration, and (d) temperature of the solution [See Clockwise].
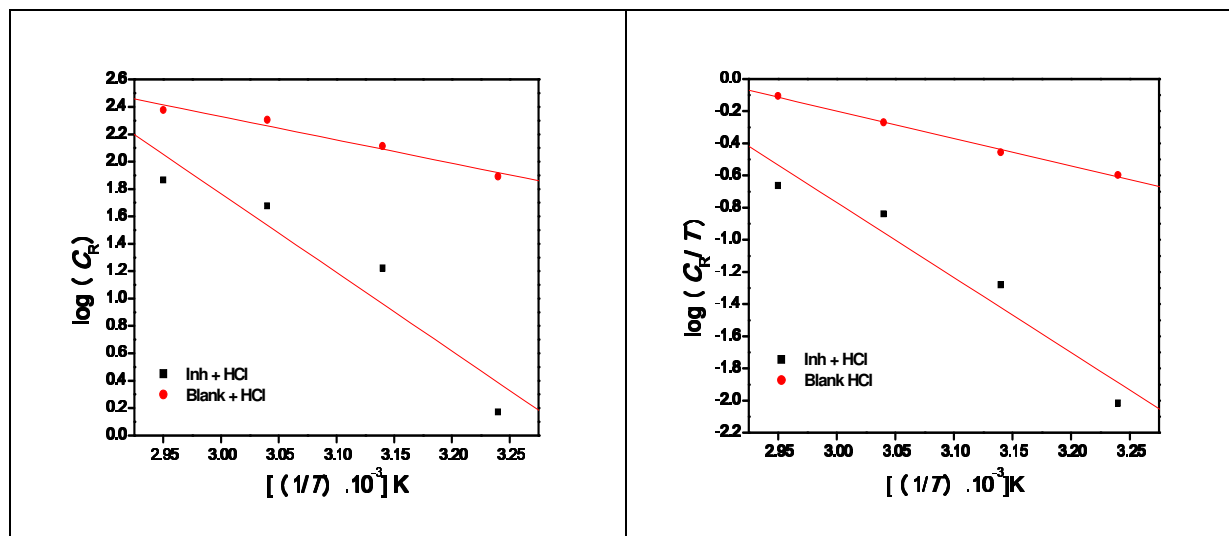
Fig.-2: Adsorption isotherm plots for (a) log C_R vs. $1/T$ and (b) log C_R/T vs. $1/T$.

(3a)

(3b)
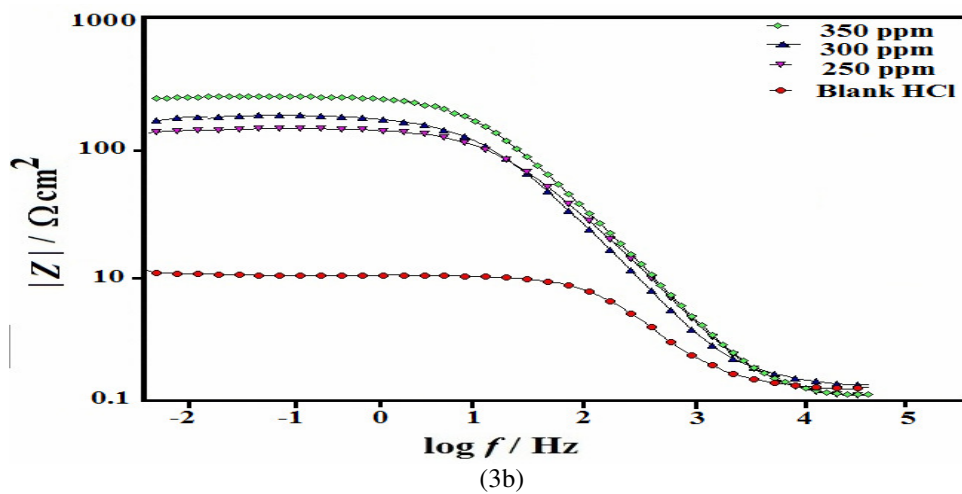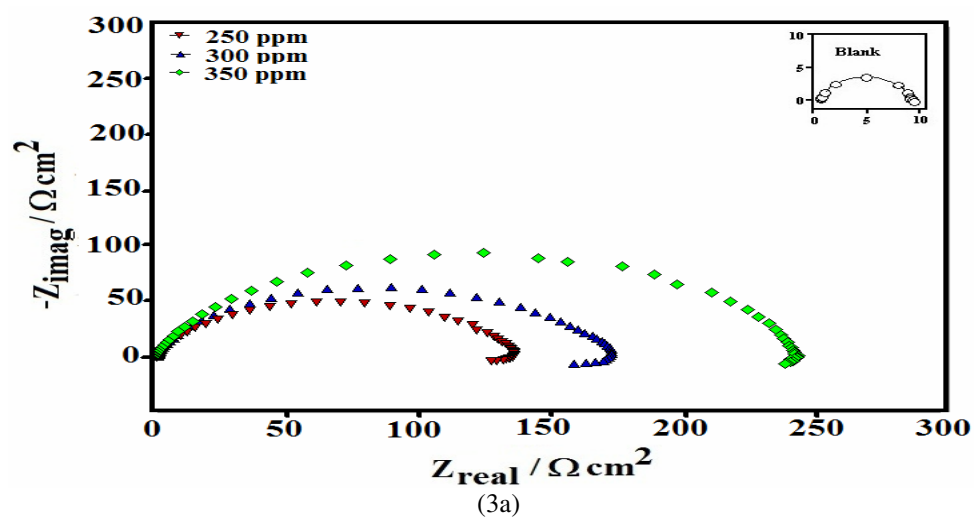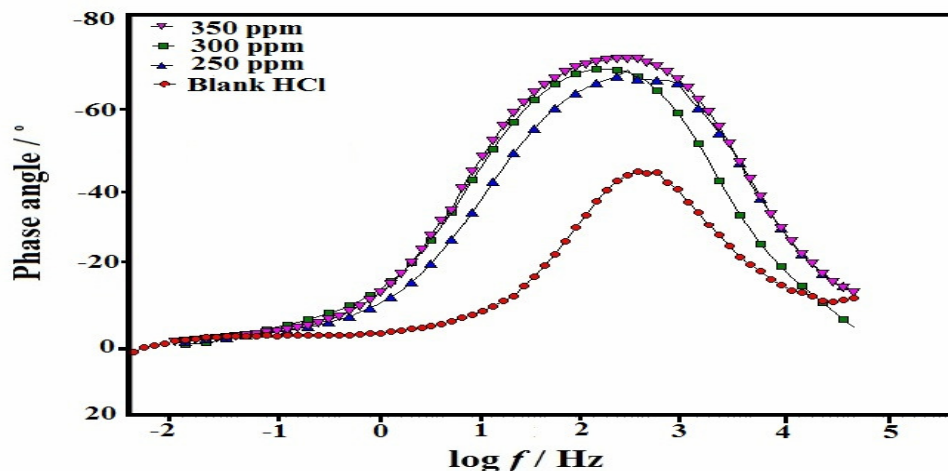
(3c)

Fig.-3: (a) Nyquist plots, (b) Bode-modulus plots, and (c) Bode-phase angle plots in absence and presence of different concentrations of extract in one molar HCl.
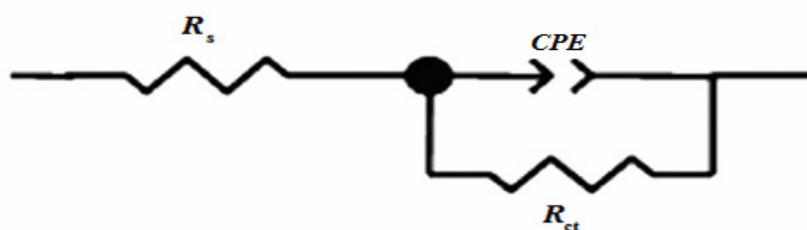
Fig.-4: Electrochemical equivalent circuit used to fit the impedance spectra.
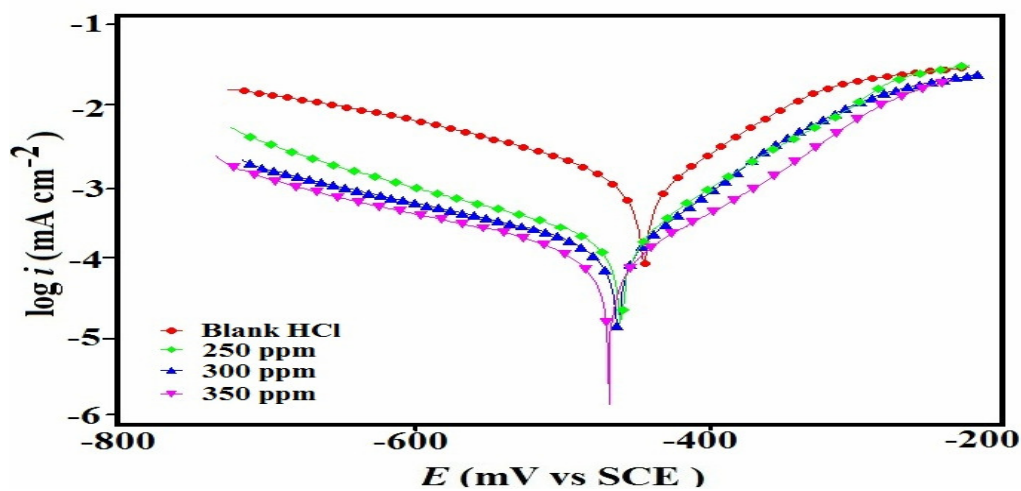
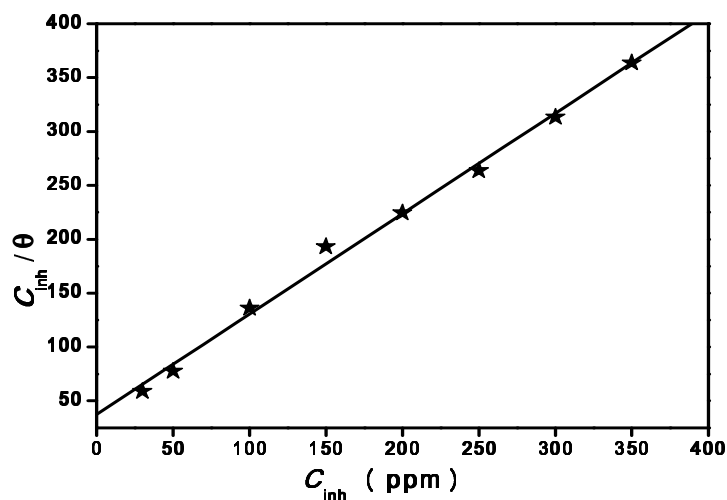Fig.-5: Polarization curves in the absence and presence of different concentrations of extract in one molar HCl.

Fig.-6: Langmuir adsorption isotherm plot for the adsorption of extract in one molar HCl on the surface of mild steel.
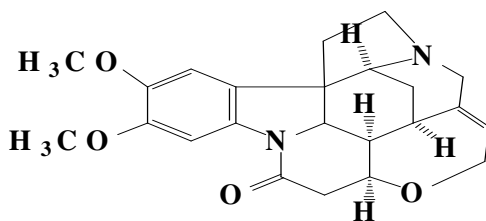
Fig.-7: Structure of main constituent of Kuchla (*Strychnos Nuxvomica*) seed extract (a) Brucine.